

## VIRTUAL INSTRUMENTS IN LOW-FREQUENCY NOISE SPECTROSCOPY EXPERIMENTS

Adam W. Stadler<sup>1</sup>, Andrzej Dziedzic<sup>2</sup>

<sup>1</sup>Department of Electronics Fundamentals, Rzeszów University of Technology, Rzeszow,  
Poland

<sup>2</sup>Faculty of Microsystem Electronics and Photonics, Wrocław University of Technology,  
Wrocław, Poland

**Abstract.** *Low-frequency noise spectroscopy (LFNS) is an experimental technique to study noise spectra, typically below 10 kHz, as a function of temperature. Results of LFNS may be presented as the 'so-called' noise maps, giving a detailed insight into fluctuating phenomena in electronic devices and materials. The authors show the usefulness of virtual instrument concept in developing and controlling the measurement setup for LFNS experiments. An example of a noise map obtained for polymer thick-film resistors (PTFRs), made of commercial compositions, for temperature range 77 K – 300 K has been shown. The experiments proved that 1/f noise caused by resistance fluctuations is the dominant noise component in the studied samples. However, the obtained noise map revealed also thermally activated noise sources. Furthermore, parameters describing noise properties of resistive materials and components have been introduced and calculated using data from LFNS. The results of the work may be useful for comparison of noise properties of different resistive materials, giving also directions for improvement of thick-film technology in order to manufacture reliable, low-noise and stable PTFRs.*

**Key words:** *low-frequency noise, noise spectroscopy, virtual instrument, polymer thick-film resistor*

### 1. INTRODUCTION

Noise measurements are much more sensitive to internal electronic component imperfections than ordinary resistance measurements since noise and resistance are proportional to the fourth and second moments of local current distribution, respectively. Taking into account that a reduction of supply voltage in modern electronic circuits is a common trend forced by commercial applications, one may realize that the noise generated in electronic components becomes one of their most important parameter. It is also observed in specialized electronics, like cryogenic thermometry, where intrinsic noise of the device limits capabilities or the resolution of the overall circuit. On the other hand, it

---

Received October 30, 2014

**Corresponding author:** Adam W. Stadler

Rzeszow University of Technology, Department of Electronics Fundamentals, W. Pola 2, PL 35-959 Rzeszow, Poland  
(e-mail: astadler@prz.edu.pl)

has been also shown that there is a relationship between low-frequency noise observed in electronic components and their reliability [1, 2]. Therefore, the noise measurements are very important research and diagnostic tool. However, noise measurements requires much more sophisticated equipment and are time consuming, as compared to resistance (or conductivity) and I-V curve tests.

It is a good practice to start noise studies with noise components identification which means that the shape of noise spectrum and its dependence on the excitation signal has to be known. One of noise components commonly observed in low-frequency range is  $1/f$  noise. However, in many electronic components, apart from  $1/f$ , other noise components may also be detected. A good example are thick-film resistors (TFRs), in which the resistive layer of  $\text{RuO}_2$ +glass is prepared in a high-temperature process, i.e., made of pastes deposited on the proper substrate and then fired in temperature of about 850 °C. In these resistors, apart from the dominant  $1/f$  noise, Lorentzian components, caused by thermally activated noise sources (TANSs) distributed randomly in the resistive layer, have also been found [3]. However, to detect TANSs and study their properties noise spectra have to be measured as a function of temperature. This research technique is called low-frequency noise spectroscopy (LFNS). Noise spectra vs. temperature have been investigated in TFRs at fixed temperature points [4], whereas LFNS used in [3, 5, 6] make it possible to depict a large amount of experimental data in the plot of fluctuating quantity vs. frequency  $f$  and temperature  $T$ , called ‘noise map’. It was possible due to continuous acquisition of voltage fluctuations observed on TFRs with the current excitation, and recording calculated in real-time consecutive spectra during slowly varying temperature. The progress was made also due to the usage of software defined instruments for controlling the experiment and processing the data. The software that supports the experiment uses virtual instrument (VI) concept, which means that the instrument consists of three main components: (i) general purpose personal computer, (ii) specialized software which is responsible for interaction with the user by means of graphical interface, and (iii) internal and/or external functional hardware (DAQ board/device, digital meters with remote control, etc.) [7, 8]. Due to the synergy, the functionality and possibilities of VIs result in equal parts both from the software and the hardware. In this work we describe in more detail the software layer that is used in studies of noise properties of electronic materials and components in function of temperature. The usefulness of VIs, developed for supporting LFNS experiments, will be shown with the use of polymer thick-film resistors (PTFRs) as the subject of studies.

## 2. ROLE OF THE SOFTWARE

As a base Noise Signal Analyzer described in [9] has been reused. The hardware part of VI is shown in Fig. 1. The heart of the system is multi-channel plug-in DAQ board, which simultaneously digitizes analog signals.

Voltage signals, including fluctuations of interest, from the multi-terminal electronic component, after conditioning are sampled and converted to digital representation giving  $2^{20}$  samples in each time record of  $t_{rec} = 2$  s duration. After spectra and/or cross-spectra calculations, executed in real-time by the use of FFT algorithm, they are displayed and certain low parts of the spectra are recorded. Additional digital voltmeters (3458A and 34410A both from Agilent) and temperature controller (Lake Shore 340) are used for monitoring biasing conditions of the sample as well as its temperature. In order to precisely

tune sampling frequency an external generator (Agilent 33120A with extended stability) is used for triggering DAQ board. All auxiliary instruments are recognized automatically at the start of the system and then exchange messages with PC controller via GPIB or USB bus.

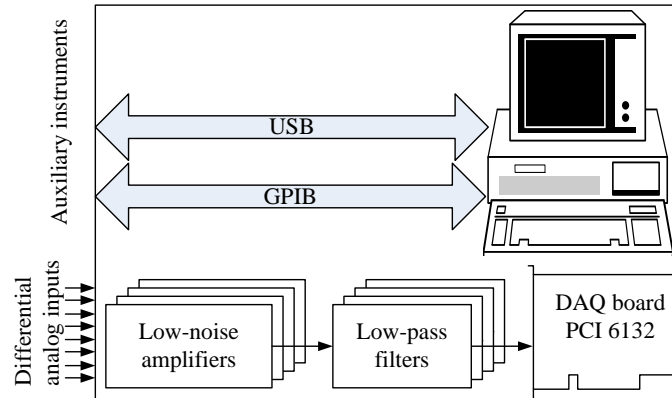


**Fig. 1** Hardware part of VI used in low-frequency noise experiments

The software part has been prepared in LabVIEW environment and is divided into two main parts: (A) controlling the experiment, and (B) post-experiment analysis. The following main tasks are defined in part (A): (i) signal sampling in continuous mode, (ii) digital signal processing of the sampled signal (in real time), including spectra calculations, (iii) monitoring resistance  $R$  of the sample and its temperature  $T$ , (iv) spectra presentation and recording together with additional data ( $R$  and  $T$ ) for further analysis. The above tasks are executed iteratively in independently running threads. The software part responsible for digital signal processing also offers more advanced functions for analysis either in time or frequency domain, like (i) phase sensitive detection (for ac method of noise measurements), (ii) detrend function [10] for removing trend and thus rejecting distortion of noise spectrum due to the temperature drift, (iii) power cross-spectral density function, which apart from ordinary power spectral density function is the most useful in experiments that involve multi-terminal samples, (iv) correlation function, (v) second spectra, etc. The complexity of the software may be expressed as a number of sub-VIs, which is about 500 for part (A) and 270 for part (B) of the software.

The block diagram of the software part of considered VI is shown in Fig. 2, where three main pieces are visible: configuration, experiment control and monitoring, and post-experiment data processing. Furthermore, three traditional layers, i.e. hardware (acquisition), analysis and presentation, have been shown in the background of experiment control. Under the hood, during the experiment several loops are executed concurrently in separate threads which communicate with each other via queues. The first loop acquires data from DAQ board and passes them to digital signal processing engine that calculates, selected previously at the configuration stage, functions in time and/or frequency domain. Another loop continuously reads measurements from auxiliary meters and calculates actual resistance and temperature. Loops interacting with hardware functional blocks, i.e. DAQ-board/device and monitors/controllers, iterate independently with their own pace. For transferring data between loops, an advanced queues mechanism has been employed, not

to lose any time record and results of calculated functions. Averaging engines have been used for data decimation during the experiment with the way and rate configured by the user.

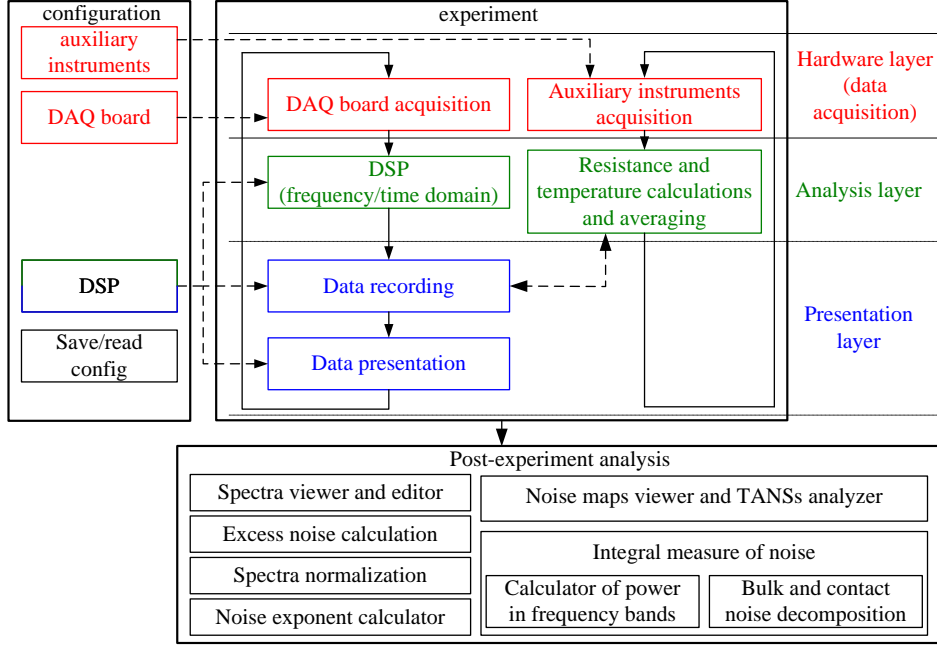


**Fig. 2** Block diagram of the software part of VI developed to support low-frequency noise spectroscopy

LFNS experiment takes long time, which is the result of small rate of temperature changes. Namely, to avoid spectra distortion due to the temperature drift, the following relation has to be fulfilled [11]

$$\alpha t_{rec} / (2\pi^2 f^2) \ll S_{Vex}(f), \quad (1)$$

where  $\alpha$  is the rate of voltage drift caused by temperature change, and  $S_{Vex}$  is excess noise,  $S_{Vex} = S_V - S_{V=0}$ , where  $S_V$  and  $S_{V=0}$  are power spectral densities of voltage fluctuations with bias and with no sample bias, respectively. However, if the above relation is not fulfilled, then the spectra will include distortion (mainly in low-frequency range) obscuring the useful information. Nevertheless, the negative influence of the resistance drift, may be significantly reduced by using detrend procedure, which removes unwanted small changes in the signal just before calculating spectra [11]. The above issues limit the rate of temperature changes and therefore the temperature sweep in the experiment covering temperature range 77 K – 300 K lasts nearly 2 days. During this time, consecutive time records, acquired from the device under test, are used for (cross)spectra calculations. It means that about 86 thousands of spectra, each counting 1000 (or even more) bins for every acquired signal have to be decimated and recorded in separate files. Hence, the software support for post-experiment data processing is necessary. The main progress with respect to Noise Signal Analyzer, described in [9], concerns part (B) of the software. It consists of the functions responsible for

(i) spectra viewing, editing and their transformations, including excess noise calculations, noise normalization, etc., (ii) noise maps generating and viewing, as well as TANSs identification and analysis, including calculation of activation energy, (iii) calculations of the powers of fluctuating quantity in the user defined frequency bands as a function of temperature, necessary for evaluation of the integral noise measure [3], (iv) decomposition of total noise into bulk and contact components, which is possible for multi-terminal samples, and (v) calculations parameters describing noise properties, like noise spectral exponent, material noise intensity parameter  $C$  (see next section). All the functions create graphs with plots and/or save their results in files for further analysis (see bottom part of Fig. 2).

### 3. EXPERIMENT

As a subject of studies a pair of PTFRs, with matched resistance, prepared on the same substrate, has been taken. Resistive layers of PTFRs have been made of ED7100 200 $\Omega$  - carbon-based composition from Electra Polymers Ltd on FR-4 laminate. Samples have been prepared as multi-terminal PTFRs in which rectangular resistive layer (length  $L = 15$  mm, width  $w = 0.5$  mm and thickness  $d = 20$   $\mu\text{m}$ ) ended on opposite sides with current terminals. Additional, evenly spaced along the layer, terminals (voltage probes) have also been formed. Such shape of sample has been used in our previous experiments [3]. Polymer thick-film resistive films have been screen-printed on bare Cu contacts.

The substrate with the pair of samples has been then inserted into liquid nitrogen cryostat, making lower arms of the dc bridge (see Fig. 3). Ballast resistors  $R_B$  have been selected so as to fulfil the relation  $R_B \gg R_S$ . The circuit has been supplied from programmable source measure unit (Keithley 2636) working in voltage mode and low-pass passive filter of large time constant. Signals from diagonal of the bridge and its sub-diagonals have been connected to differential low-noise preamplifiers (5186 from Signal Recovery) with 1000 gain and then after low-pass filtering digitized in acquisition plug-in board. Spectra  $S_V$  and cross-spectra (with 0.5 Hz resolution) for signals taken from samples terminals have been calculated in real time by the software and gathered in proper files for further analysis. The experiment started with cooling down the sample and letting the temperature rise freely.

It should be noted that the voltage  $V_{7-7}$  acquired from the diagonal of the bridge includes fluctuations arising in both samples. Similarly, voltages from sub-diagonals,  $V_{i-i}$ , include fluctuations that arise in both samples but only in parts of the resistive layers (sectors) marked by terminals '1' and 'i', where  $i = 2 \dots 6$ . Furthermore, in order to obtain voltages from sectors 3-5 and 2-6 covering internal sectors of the resistive layer, voltages  $V_{5-5}$ - $V_{3-3}$  and  $V_{6-6}$ - $V_{2-2}$  have been created by the use of amplifiers/filters with differential inputs. To improve the accuracy of the spectra calculation for the internal sectors, cross-correlation technique has been employed, i.e. cross-power spectral density function has been used for calculation  $S_{V(1-i)}$  using voltages  $V_{7-7}$  and  $V_{i-i}$ , while  $S_{V(1-7)}$  has been calculated using ordinary power spectral density function from voltage  $V_{7-7}$ . Due to the advantage of the method [6],  $S_{V(1-6)}$ , are free from noise of voltage probes, including both contacts noise and noise of resistive arm, although it includes (apart from noise of the part of the main resistive layer) also noise of current contacts at terminals '1'. On the other hand,  $S_{V(1-7)}$  includes noise of contacts at terminals '1' and '7' and noise of the whole resistive layers. In a similar way,  $S_{V(2-6)}$  and  $S_{V(3-5)}$  calculated as cross-power spectral density of  $V_{7-7}$  and either  $V_{5-5}$ - $V_{3-3}$  or  $V_{6-6}$ - $V_{2-2}$  are free from noise of current contacts as well as voltage probes.

During the experiment, apart from the spectra of interest, also current resistance of the sample,  $R_S$ , is calculated and recorded, using supply and sample voltages and the known value of ballast resistor  $R_B$ . Since temperature of the sample is also monitored and recorded, temperature dependence of sample resistance,  $R_{1-7}(T)$ , is also the result of LFNS experiment.

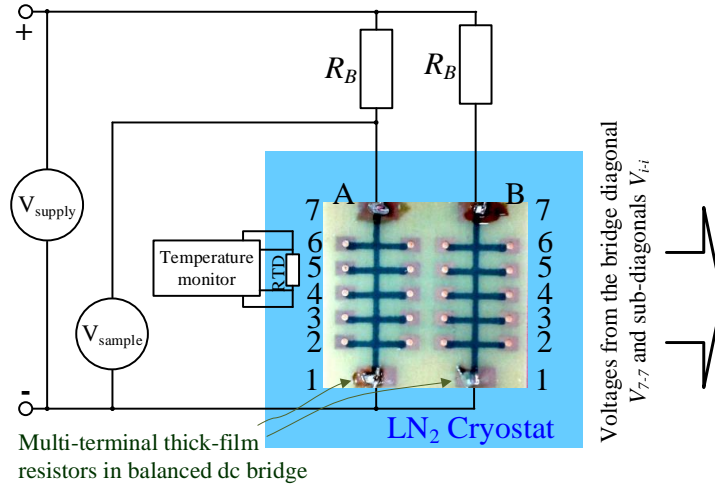


**Fig. 3** Measurement setup for noise studies in multi-terminal TFRs

#### 4. RESULTS

Entry test of samples, executed at room temperature, cover measurements of voltage distribution along the resistive layer, noise spectra measurements for identification main noise components and samples selection. The voltage distribution has been shown in Fig. 4 (points). The data points for terminals 2 – 6 have been used in a linear fit (solid line) for evaluation sheet resistance  $R_{sq} = 0.353 \text{ k}\Omega/\square$ , while the expected nominal value was  $200 \text{ }\Omega$ . From the intersections of the extrapolated line (dashed line) with coordinates, resistances of contacts may be calculated. It thus occurred that the resistance of bottom contact is  $R_{contact(1)} = 273 \text{ }\Omega$  while  $R_{contact(7)} \approx 0 \text{ }\Omega$ .

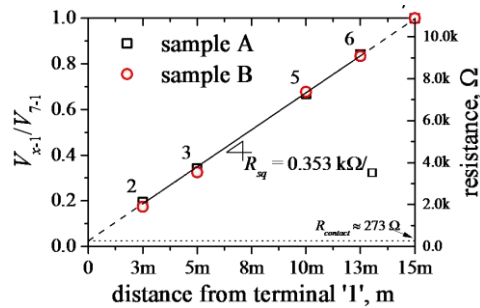


**Fig. 4** Voltage distribution along the resistive layer.  
Terminals' labels have been given near the corresponding points.

The fundamental issue in noise properties studies is the identification of noise components. To do that, spectra of fluctuating quantity (current or voltage) are acquired as the function of sample bias. It has been shown in Fig. 5a, where collection of excess noise spectra gathered at room temperature for terminals 7-7,  $S_{V_{ex}(1-7)}$  is plotted for different sample voltages. Additionally, background noise,  $S_{V=0}$ , and dashed line for pure  $1/f$  noise have been drawn for reference. It is obvious that  $1/f$  noise is dominant. Therefore, it is convenient to use product of frequency and  $S_{V_{ex}}$ ,  $\langle f \cdot S_{V_{ex}} \rangle_{\Delta f}$ , averaged over certain frequency band,  $\Delta f$ , as the measure of noise intensity. The plot of this quantity, calculated for decade frequency bands, *versus* sample voltage (points) is show in Fig. 5b. Squared voltage dependence has been added (dashed line) for reference. It is visible that the observed noise is caused by resistance fluctuations.

After tests at room temperature, the substrate with studied PTFRs has been inserted into  $LN_2$  cryostat, cooled-down and noise spectra have been recorded during warming-up. An exemplary plot of the noise map has been shown in Fig. 6. In this map the product  $f \cdot S_R$ , where  $S_R = S_{V_{ex}}/I^2$  and  $I$  is biasing current, has been plotted *vs* frequency and reciprocal temperature. Such fluctuating quantity,  $f \cdot S_R$ , has been chosen since it is sample voltage independent and other than  $1/f$  noise components are emphasized. Furthermore, reciprocal temperature scale (horizontal scale in Fig. 6) helps in direct detection of TANSs which are visible in the map as streaks, marked with dashed lines. From the slopes of these lines, activation energies of TANSs [6] have been calculated:  $E_g = 1013$  meV, 736 meV, 642 meV, 316 meV, 303 meV.

The set of TANSs visible in the noise map is sample-dependent since only those TANSs are visible that modulate resistances in the critical percolation path. Analyzing noise map of Fig. 6 we may notice that at temperatures 145 K and 186 K there are vertical streaks that look like unwanted interferences. But further inspection of noise spectra ensures that the noise map is correct and non-stationary noise sources have been recorded. Their individual spectra of Lorentzian shape have been shown in Fig. 7. Additionally, another two spectra, for intermediate temperature, including TANS of  $E_g = 303$  meV have been plotted. Furthermore, the spectrum with two Lorentzians has been also shown in Fig. 7 that has been caught at 77 K, which means that TANSs also exist in a lower temperature range.

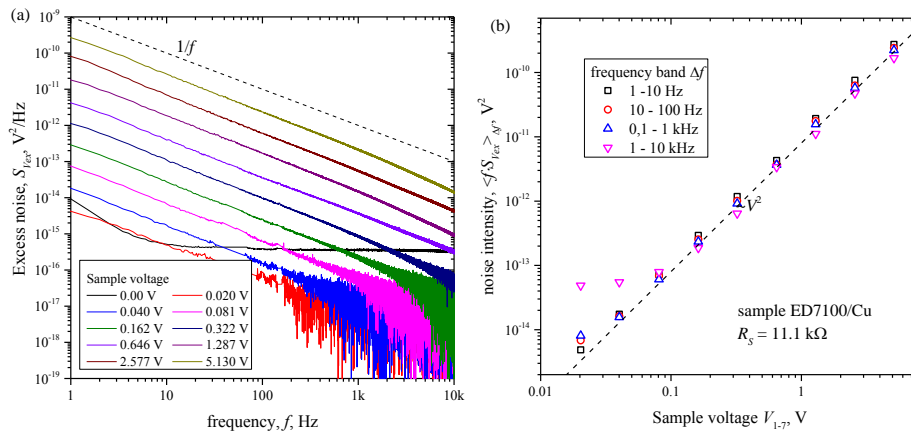


**Fig. 5** (a) Excess noise for different sample voltages.  
(b) Noise intensity *versus* sample voltage

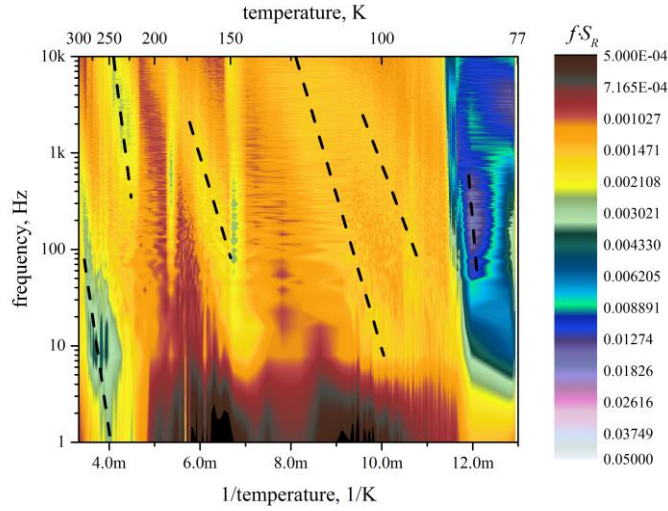


**Fig. 6** Noise spectra gathered for samples made of ED7100 with Cu contacts plotted as a noise map, i.e. the quantity  $fS_R$  versus frequency and temperature

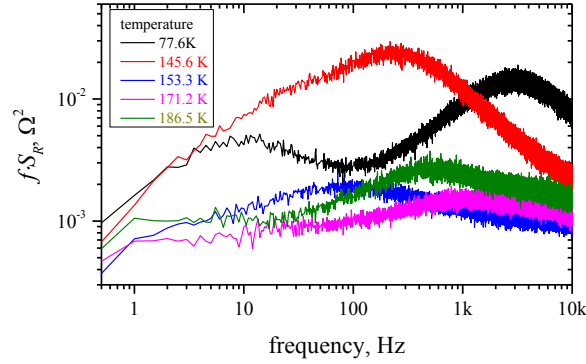


**Fig. 7** Selected spectra with visible Lorentzians

## 5. INTEGRAL NOISE MEASURE

As we can see, the dependence of noise intensity is subject to large variations, which has been shown in the noise map in Fig. 6 and also in Fig. 8. Since only those TANSs are visible in noise maps that modulate critical resistances in percolation paths, dependence of  $\delta R^2$  versus temperature is irregular, although temperature dependence of resistance, also shown in Fig. 8, is monotonic and smooth. It implies the necessity of averaging  $\delta R^2$  over temperature to obtain a reliable noise measure. Namely, having  $S_R(f, T)$  as a result of LFNS experiment, we use the integral measure of noise intensity [12]:

$$s = (T_2 - T_1)^{-1} \int_{T_1}^{T_2} \int_{f_1}^{f_2} S_R(f, T) df dT, \quad (2)$$

where  $T_1$ ,  $T_2$  and  $f_1, f_2$  determine temperature and frequency range, respectively. The inner integral calculates the power,  $\delta R^2$ , of resistance fluctuations, while the outer integral averages  $\delta R^2$  over the temperature. The plot of  $\delta R^2$ , calculated for studied resistors in decade frequency bands, has been shown in Fig. 8.

The values of integral  $s$  calculated for different sectors of the studied resistor, for frequency band 1 kHz – 10 kHz have been then used for the decomposition of the noise of the whole resistor into bulk and contact noise components, which has been depicted in Fig. 9, where  $s$  has been plotted vs sectors' size. It should be noted, that the noise of two samples/sectors is measured acquiring signals from the bridge diagonal/sub-diagonals. As the internal sectors of resistor, i.e. sectors (3-5) and (2-6), are far from current contacts also  $s$  calculated for them is free of contact noise, while  $s$  calculated for sectors (1-6) and (1-7) includes noise of bottom contacts and all contacts, respectively. Hence, from the slope of linear fit of  $s$  for sectors (3-5) and (2-6) we obtain 's per square',  $s_{sq} = 1.4 \cdot 10^{-5} \Omega^2$ . Next, dimension-independent bulk noise intensity  $C_{bulk} \equiv s_{sq} / R_{sq}^2 \times \Omega_{sq}$ , is calculated:  $C_{bulk} = 5.7 \cdot 10^{-22} \text{ m}^3$ , where  $\Omega_{sq}$  is the volume of the individual square [12]. Parameter  $C_{bulk}$  occurred to be very helpful for comparison noise properties of different materials [12-14].

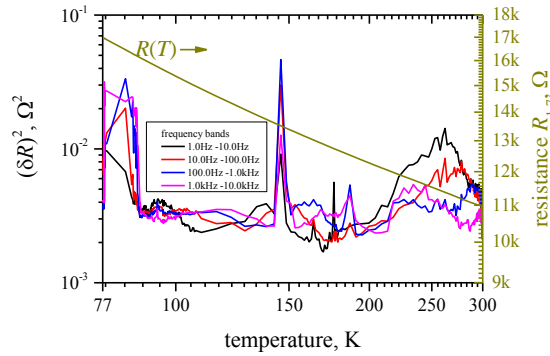


**Fig. 8** Power of resistance fluctuations versus temperature and temperature dependence of resistance

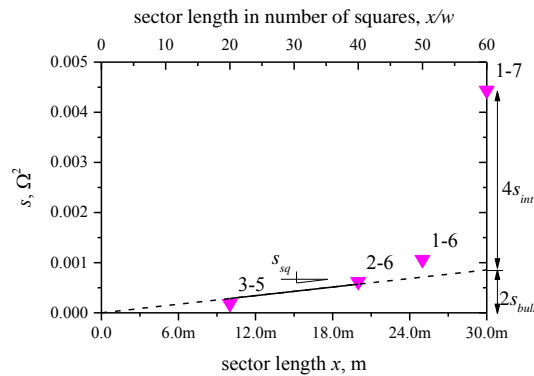


**Fig. 9** The integral  $s$  versus sector size (points). Sectors are labelled near data points. Solid line is the linear fit of data corresponding internal sectors of the resistor (labelled (3-5) and (2-6)), while dashed line is its extrapolation

The noise generated in the interfaces of both current contacts can be evaluated as a difference between noise intensity measured for the whole resistor,  $s_{1-7}$ , and extrapolated bulk noise  $s_{bulk} = L/w \times s_{sq}$ , which is depicted in Fig. 9. Analyzing the plot of Fig. 9 we can see that the noise generated in contacts at the terminals ‘7’ significantly contributes to the overall noise. To compare the quality of the interface we use contact-geometry-independent parameter,  $C_{int} \equiv ws_{int}/s_{sq}$  [12]. Its numerical value is the length of hypothetical resistive film, which would have the noise intensity equal the intensity of the interface noise. In this case, we obtain  $C_{int} = 32$  mm, which means that the quality of the interface between resistive layer and Cu contacts is very poor and the contribution of noise contacts in the noise of the resistor is significant.

The main reason for the introduction of parameters describing noise properties is to make possible quantitative comparison of the noise properties of different materials or devices. An example is the current noise index (CNI) defined for resistors or resistive materials [15 Method 308] and often used by the manufacturers. However, CNI is useless in characterization of materials properties as long as geometrical dimensions of the samples are unknown. Therefore, another parameter is introduced, i.e. material noise intensity,

$$C \equiv \Omega f S_R / R^2, \quad (2)$$

where  $\Omega$  is the volume of the sample. It is worth to note that  $C$  describes properties of the material itself, since it is frequency, as well as sample volume and bias independent. Hence, parameter  $C$  describes properties of samples with various geometry and therefore is considered as the most proper quantity for materials characterization with respect to  $1/f$  noise [16]. Furthermore, using the value of  $C$  and geometrical dimensions of the sample it is possible to calculate measurable quantity, i.e. power spectral density of voltage or current fluctuations for the known bias. The parameter  $C$  is equivalent to the previously defined  $C_{bulk}$ , however,  $C_{bulk} = C \ln 10$ . The value  $C = 2.5 \cdot 10^{-22} \text{ m}^3$  obtained for studied in this work resistive layer of ED7100 is very close to  $10^{-21} \text{ m}^3$  found in [17] for squared resistors (size 1.5 mm) of ED7100 with Cu contacts but it is still more than 1 order of magnitude larger than  $C \approx 0.6 \cdot 10^{-23} \text{ m}^3$  found for Pb-rich  $\text{RuO}_2$ +glass thick-film layers [3].

## 6. SUMMARY

The importance of the software support in low-frequency noise spectroscopy has been explained. Virtual Instrument concept and its usage in controlling LFNS experiment and post-experiment data processing have been described. Since the functionality and possibilities of VIs result in equal parts both from software and hardware, it is easy to expand the capabilities of VIs by changing existing or developing new sub-VIs.

As the subject of LFNS experiment, that showed the usefulness of VI concept, PTFR of ED7100 resistive ink with Cu contacts has been used. The shape of test resistor was multi-terminal allowing for (i) studies of noise vs volume of the sample, and (ii) localization of noise sources in different parts of the resistor, (iii) obtaining valuable information concerning the quality of the interface resistive/conductive layer. The experiments proved that  $1/f$  noise caused by resistance fluctuations is the dominant noise component in the studied samples. However, exemplary noise map as the result of LFNS, revealed also thermally activated noise sources. The noise map gave detailed insight into fluctuating

phenomena and opened the door for introduction of integral noise measure. Parameters used for characterization of noise properties of resistive materials and components, including material noise intensity  $C_{bulk}$  and  $C_{int}$  describing the quality of the interface between resistive and conductive layers in TFR, have been defined and calculated for studied samples. It has been found that interface between polymer composition ED7100 and Cu contacts has very poor noise properties.

The concepts shown in this work may also be used for studies of noise properties in other electronic components, both passive and active. The results obtained by LFNS may be utilized in thick-film technology in selection materials for manufacturing low-noise, reliable resistive components with stable parameters as well as in improvements of the technology in order to achieve technological advantage.

**Acknowledgement:** *The work has been supported from Grant DEC-2011/01/B/ST7/06564 funded by National Science Centre (Poland) and from Rzeszow University of Technology Project U-235/DS. Studies have been performed with the use of equipment purchased in the project No POPW.01.03.00-18-012/09 from the Structural Funds, The Development of Eastern Poland Operational Programme co-financed by the European Union, the European Regional Development Fund.*

#### REFERENCES

- [1] D. Rocak, D. Belavic, M. Hrovat, J. Sikula, P. Koktavy, J. Pavelka, V. Sedlakova, "Low-frequency noise of thick-film resistors as quality and reliability indicator", *Microelectronics Reliab.*, vol. 41, pp. 531-542, 2002.
- [2] L.K.J. Vandamme, "Noise as a diagnostic tool for quality and reliability of electronic devices", *IEEE Transactions on Electron Devices*, vol. 41, pp. 2176-2187, 1994.
- [3] A.W. Stadler, "Noise properties of thick-film resistors in extended temperature range", *Microelectronics Reliab.*, vol. 51, pp. 1264-1270, 2011.
- [4] B. Pellegrini, R.Saletti, P. Terreni, M. Prudenziati, " $1/f^{\alpha}$  noise in thick-film resistors as an effect of tunnel and thermally activated emissions, from measures versus frequency and temperature", *Phys. Rev. B*, vol. 27, pp. 1233-1243, 1983.
- [5] A.W. Stadler, A. Kolek, Z. Zawislak, K. Mleczo, M. Jakubowska, K.R. Kielbasiński, A. Mložniak, "Noise properties of Pb/Cd-free thick film resistors", *J. Phys. D: Applied Physics*, vol. 43 (26), 265401 (9pp), 2010.
- [6] A. Kolek, A.W. Stadler, P. Ptak, Z. Zawislak, K. Mleczo, P. Szalański, D. Żak, "Low-frequency  $1/f$  noise of RuO<sub>2</sub>-glass thick resistive films", *J. Appl. Phys.*, vol. 102, 103718 (9pp), 2007.
- [7] H. Goldberg, "What is virtual instrument", *IEEE Instrumentation & Measurement Magazine*, vol. 3, No. 4, pp. 10-13, 2000.
- [8] P. Janković, J. Manojlović, S. Đukić, "Virtual Instrumentation for Strain Measurement using Wheatston Bridge Model", *Facta Universitatis, Series: Elec. Energ.*, vol. 26, No 1, pp. 69 – 78, April 2013.
- [9] A.W. Stadler, "Noise signal analyzer for multi-terminal devices", In Proceedings of the 31st Int. Conf. of IMAPS Poland Chapter, Rzeszów - Krasiczyn, Poland, 2007, pp. 413-416.
- [10] LabVIEW 2013 Advanced Signal Processing Toolkit Help, [http://zone.ni.com/reference/en-XX/help/372656C-01/lvtimeseriestk/tsa\\_de-trend/](http://zone.ni.com/reference/en-XX/help/372656C-01/lvtimeseriestk/tsa_de-trend/)
- [11] A. Kolek, *Experimental methods of low-frequency noise* (In Polish). Rzeszow, Poland: Rzeszow University of Technology Publishing House, 2006.
- [12] K. Mleczo, Z. Zawislak, A.W. Stadler, A. Kolek, A. Dziedzic, J. Cichosz, "Evaluation of conductive-to-resistive layers interaction in thick-film resistors", *Microelectronics Reliab.*, vol. 48, pp. 881-885, 2008.
- [13] A. Kolek, P. Ptak, A. Dziedzic, "Noise characteristics of resistors buried in low-temperature co-fired ceramics", *J. Phys. D: Applied Physics*, vol. 36, pp. 1009-1017, 2003.

- [14] L.K.J. Vandamme, H.J. Casier, "The  $1/f$  noise versus sheet resistance in poly-Si is similar to poly-SiGe resistors and Au-layers", In Proceedings of the Proc 34th European solid-state device research conf (Leuven, Belgium), 2004, p 21.
- [15] Test Method Standard Electronic and Electrical Component Parts, MIL-STD-202G, 2002.
- [16] A. Dziedzic, A. Kolek, " $1/f$  noise in polymer thick-film resistors", *J. Phys. D: Applied Physics*, vol. 31, No. 17, pp. 2091-2097, 1998.
- [17] A.W. Stadler, Z. Zawislak, A. Dziedzic, W. Stęplewski, "Studies of noise in polymer thick-film resistors embedded in printed circuit boards", In: *Microelectronic Materials and Technologies* (Ed. by Zbigniew Suszyński), Koszalin Technical University Monograph Series – Monograph No. 231, Koszalin 2012, vol. 1, pp. 82-97.